

Evaluation of microstructure and transport properties of hydrating cement paste using micro-CT image

¹Zhang MZ^{1*}

¹ Microlab, Faculty of Civil Engineering and Geosciences, Delft University of Technology, Stevinweg 1, 2628 CN Delft, The Netherlands

²He YJ

² Key Laboratory for Silicate Materials Science and Engineering, Wuhan University of Technology, Wuhan 430070, China

¹Ye G, ³Lange DA, ¹van Breugel K

³ 2129 Newmark Civil Engineering Laboratory, University of Illinois, 205N. Mathews, Urbana, IL, USA, 61801-2352

Abstract

X-ray computed microtomography (micro-CT) was utilized to obtain three-dimensional (3D) images of the hydrating of cement paste with water-to-cement (w/c) ratio at different ages, i.e., 1, 3, 7 and 28 days. On the basis of the gray level histogram of microtomography images, the phase threshold values for each specimen were determined. The component phases of the cement paste such as pores, hydration products and unhydrated cement particles were identified from each other. The volume fraction of pore and degree of hydration of the specimens at different curing ages were estimated from the image analysis and compared with the experimental data measured by mercury intrusion porosimetry (MIP) tests and loss-on-ignition (LOI) tests respectively. Furthermore, the degree of pore connectivity was analyzed based on cluster-labelling technique. Finally, transport properties, e.g. diffusivity of tritiated water of each specimen was estimated and compared with the experimental results obtained from the literature. The results derived from image analysis show a reasonably agreement with the measured results, which indicates that micro-CT is a reliable and suitable technique to characterize the microstructure evolution of hydrating cement paste. The obtained microstructure can be used to estimate the transport properties of cement-based materials.

Originality

X-ray computed microtomography as an innovative and non-invasive 3D imaging technique is utilized to acquire the 3D microtomography images of hydrating cement paste by second author of this study. The spatial resolution is 0.5 $\mu\text{m}/\text{voxel}$. To our knowledge, it is the highest resolution of lab-based CT image in the study of cement-based materials up to now. Based on the microtomography images, the image analysis is carried out. The estimated characteristics of hydrating cement paste such as porosity and degree of hydration are validated with the experimental results. In addition, the relationship between the measured microstructure and transport property of hydrating cement paste is studied.

Chief contributions

In view of the crucial importance of transport properties of cement paste to the durability assessment and design of cement-based materials, it is of great practical significance to predict the transport properties. Transport properties are intimately related to the microstructure. Therefore, it is of importance to investigate the microstructure of cement paste firstly. The study presented herein represents the measured microstructure by using X-ray microtomography at a high spatial resolution. Furthermore, the microstructure-based prediction of transport properties of cement paste is carried out. The predicted results can be used as input to determine the transport properties of mesoscale mortar/concrete based on the further unpscale modeling and used by civil engineers and designers to assess the durability and predict the service life of structures.

Keywords: X-ray computed microtomography, Microstructure, Transport property, Cement paste

¹ Corresponding author: Email m.zhang@tudelft.nl Tel +31(0)152782868 Fax +31(0)152786383

1. Introduction

Transport properties of cement paste play a critical role in the durability design and assessment of cement-based materials. They are intimately related to the microstructure of cement paste, especially the pore structure characteristics. Analysis and quantification of the pore structure in three-dimension (3D) will help us a better understanding of transport phenomena in cement-based materials. In recent years, the 3D X-ray computed microtomography (micro-CT) was applied in the study of cement-based materials [Promentilla 2009, Rougelot 2010]. X-ray micro-CT is a non-invasive and non-destructive imaging technique that is based on the absorption dependency of X-rays on material density, atomic number of the chemical components of the material and the energy and power of the CT machine. The major disadvantages of micro-CT scanning are the limitations in spatial resolution and temporal resolution and distinction between components of the materials having similar attenuation coefficients. With the recent development of micro-CT scanning, the spatial image resolution for the research of cement-based materials could be as high as $0.5\text{ }\mu\text{m/voxel}$. Although the resolution may be not sufficient, it will provide us new information about the evolution of 3D microstructure, especially the pore structure of cement-based materials.

In this study, X-ray micro-CT is applied to obtain three-dimensional (3D) images of hydrating Portland cement paste specimens with water-to-cement (w/c) ratio 0.5 at different curing ages. The spatial resolution of images is $0.5\text{ }\mu\text{m/voxel}$. On the basis of image analysis, the 3D microstructure of hydrating cement paste consisting of pores, hydration products and unhydrated cement particles are identified and the reconstructed microstructure characteristics such as porosity and degree of hydration are investigated. Furthermore, the diffusion process of tritiated water through the reconstructed 3D microstructure is simulated by means of finite element method (FEM). Based on Fick's law, the effective diffusion coefficients of tritiated water is estimated.

2. Experiments and methods

2.1. Experiments description

The cement used was Portland cement (ASTM type I). The w/c ratio of the paste is 0.5 (mass basis). The sample was cured in a standard curing room (a relative humidity of 95% and a temperature of $20\text{ }^{\circ}\text{C}$) for 1, 3, 7 and 28 days, which are referred here as OPC_1d, OPC_3d, OPC_7d and OPC_28d respectively.

X-ray micro-CT testing was performed at the Beckman Institute for Advanced Science and Technology of University of Illinois at Urbana-Champaign (UIUC). Firstly, the cement paste was poured into the syringe. Secondly, the steel needle of the syringe was prior pulled out and replaced with a $250\text{ }\mu\text{m}$ micro plastic tube and the plastic tube was adhered tightly on the syringe with super glue. Finally, the fresh cement paste was injected into the micro plastic tube by gently pushing the piston of the syringe. Details of this experimental procedure were described in a previous paper [He 2010].

The degree of hydration can be expressed as the ratio of the non-evaporable water content per gram cement to the maximum amount of non-evaporable water at complete hydration, which is assumed to be equal to 0.23g/g for OPC. In this study, Loss-on-ignition (LOI) test [Feng 2004] was carried out to measure the non-evaporable water content of the hydration specimen at certain age.

2.2. Image processing and analysis

The original X-ray projections received by the CCD detector of CT machine were converted to digital signals and stored in the computer as a data matrix. The data matrix was then reconstructed by the Xradia Reconstruction software with the algebraic method. In the image, the grayscale value of each voxel is proportional to the density of the corresponding material at that point in space. From authors' previous study, it has been presented that the representative elementary volume (REV) for diffusivity

in cement paste is $100 \times 100 \times 100 \mu\text{m}^3$ [Zhang 2010]. In order to reduce the computing time and avoid the possible edge effects, a cubic volume of interest (VOI) of $100 \times 100 \times 100 \mu\text{m}^3$ (200^3 voxels) is extracted from the center of the images where the cement paste is considered to be the most homogeneous for further image analysis.

After the acquisition of 3D reconstructed image of VOI, the image analysis is carried out to segment the images into a number of distinct categories corresponding to various particular phases of cement paste, i.e. pores, hydration products and unhydrated cement particles. In the present study, a global thresholding method, the most frequently used technique for image segmentation, is applied to differentiate the pore space and solid matrix (hydration products and unhydrated cement particles). Global thresholding is to scan each voxel in the image and determine a threshold value, below or equal to which voxels are considered to be pore phase and above which they are regarded to belong to solid phase (hydration product and unhydrated cement particles). As regards the choice of the threshold, the grayscale level histogram is usually used. An example of gray-level histogram for VOI is shown in Figure 1. In the following section, we will use this image data as a typical example to illustrate the analysis procedure. It can be seen that there are two peaks which correspond to the hydration product and unhydrated cement particle respectively. However, the segmentation of pore and hydration product is not clear.

The volume fraction of unhydrated cement ϕ_{un} can be evaluated from the data by defining a hydration product/unhydrated cement threshold to separate the phase of unhydrated cement and hydration product. The degree of hydration can be estimated on the basis of the volume fraction of unhydrated cement ϕ_{un} and the well-known Powers model, where the volume fractions of unhydrated cement ϕ_{un} is a function of the initial w/c ratio and the current degree of hydration α , as expressed:

$$\phi_{un} = (0.32 - 0.32\alpha) / (w/c + 0.32) \quad (1)$$

For instance, as shown in Figure 1, the gray level corresponding to the transition point (T_1) between the two peaks is considered as hydration product/unhydrated cement particle phase threshold. The corresponding volume fraction of unhydrated cement $\phi_{un} = (1 - 0.8529) = 0.1471$ results in a degree of hydration $\alpha = 0.6231$.

In addition, the transition point (T_2) in the curve of volume fraction change against grayscale level change is selected to be pore/hydration product phase threshold where the segmented volume fraction starts to change sharply with the increase of grayscale value.

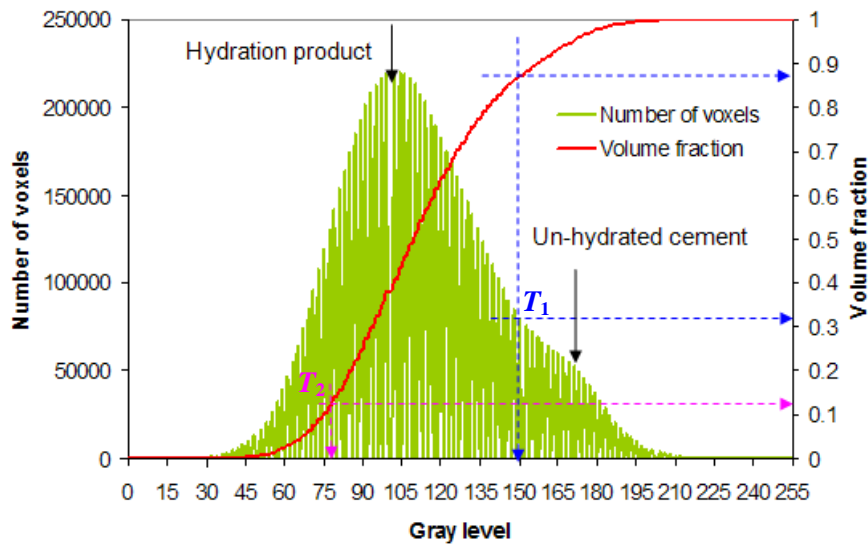


Figure 1: Example of image segmentation based on gray-level histogram

The connectivity is one of the most important characteristics for pore structure of cement paste. After pore segmentation, a home-made program Perc_3d on the basis of cluster-labeling algorithm proposed by Hoshen and Kopelman [Hoshen 1976] is applied to analyze the connectivity of pore voxels. More detailed information about this procedure is listed in Ref [Zhang 2010]. After the cluster-labeling is complete, the labeled voxels that are not connected to both ends of specimen (x-, y- and z-axis) are identified to be isolated pores. The degree of pore connectivity is defined as the volume fraction of the labeled pore voxels that are connected to both ends of specimen. A degree of pore connectivity of one means that all the pore voxels are interconnected to each other. Otherwise, a degree of pore connectivity of zero demonstrates that disconnection happens in at least one direction of the specimen. The connected porosity can be estimated by multiplying the degree of pore connectivity to volume fraction of pore voxels.

2.3. Transport properties

Based on the reconstructed microstructure, the transport properties of the hydrating cement paste can be investigated. Due to the limited space, in the present study, the diffusion process of tritiated water through cement paste simulated by means of finite element method (FEM) is taken as an example. Tritiated water is chosen as solute for simulation because of the negligible chemical interactions of this type of water with the cement hydrates. Each voxel of the reconstructed microstructure is converted into corresponding finite element. Water transport is dominated by the capillary pores as long as they form continuous pathway. In the simulation, only the diffusion of tritiated water through capillary pores is taken into account. The diffusion coefficient of tritiated water through capillary pores was assumed to be $2.05 \times 10^{-9} \text{ m}^2/\text{s}$ (at 20 °C) [Mills 1973].

In experimental investigations, a two-compartment diffusion cell test is commonly used to determine the diffusion coefficient of tritiated water in cement paste. Similar to the experiments, a procedure to simulate diffusion cell test is performed. The concentration on the upstream compartment C_1 is kept constant during the simulation (in this study, it is 1 M, i.e., 1 mol/l). In addition, C_1 is chosen much larger than the concentration on the downstream compartment C_2 . In the simulation, C_2 is chosen to be zero. In addition, the initial concentration in cement paste is assumed to be zero. The concentration gradient leads to a flux of tritiated water across the specimen, with the flow migrating to the downstream surface and ultimately reaching the steady state. The flow Q in all the elements lying on the downstream surface is summed. The flux J across the entire microstructure is obtained by dividing the flow Q by the area of the cross-section A . The value is then used in accordance with Fick's first law to estimate the effective diffusion coefficient of tritiated water through hydrating cement paste. Detailed procedure is explained in a prior paper [Zhang 2010].

3. Results and discussions

Figure 2a) shows a cross sectional X-ray CT image of the specimen OPC_3d with a diameter of 250 μm . The corresponding VOI is shown in Figure 2b). In the 8-bit grayscale image, each voxel takes on a value ranging from 0 to 255. In this case, 0 is black corresponding to minimum density (pores). 255 is white corresponding to maximum density (unhydrated cement particles).

By choosing the threshold value on the basis of the method mentioned above, the pores, hydration products and unhydrated cement particles can be identified from each other. Accordingly, the 3D microstructure of VOI of each specimen can be reconstructed, as shown in Figure 3a) ~ d). One can see that with the increase of the curing age, the capillary pores (blue voxels) are gradually filled by hydration products. The hydration products (grey voxels) appear first around the cement particles and then spread to the available space in capillary pores. It is quite obvious during the first three days. The unhydrated cement particles (dark red voxels) become smaller and fewer. Figure 4 illustrates the evolution of volume fraction of the pores, the hydration products and the unhydrated cement particles. The total porosity of cement paste estimated from mercury intrusion porosimetry (MIP) test [Raymond 1999] is also plotted in Figure 4 for comparison. Even though the porosity derived from MIP test is

somewhat higher than the volume fraction of pores from μ CT image analysis. However, the trend of the evolution of the porosity shows a good agreement. The difference in porosity is likely attributed to the spatial resolution of microtomography images. In this study, the spatial image resolution is $0.5\text{ }\mu\text{m/voxel}$. As a consequence, the pore space smaller than $0.5\text{ }\mu\text{m}$ are not detected and will be identified as a part of hydration products. However, the trend of porosity evolving with curing age based on μ CT image data shows a good agreement with that measured by MIP test. Comparing with MIP test method, the advantage of using micro-CT scanning is that the dimensional distribution of the pores and their connectivity can be characterized.

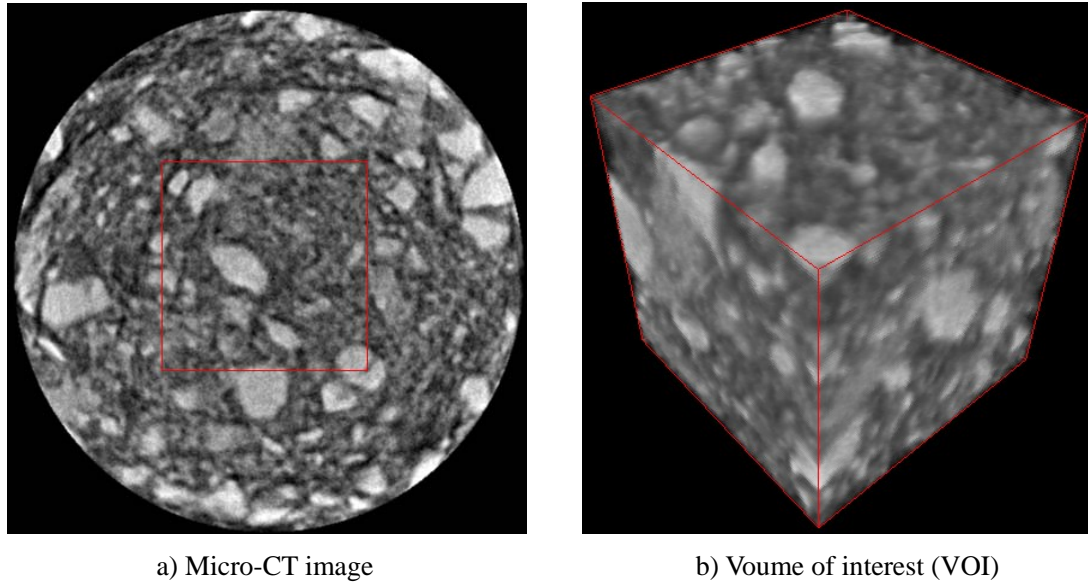


Figure 2: An example cross sectional X-ray microtomography image and corresponding VOI

Figure 5 gives the degree of hydration of cement paste as a function of curing age, which is compared with the experimental results measured by LOI test. It can be seen that there is a relatively good agreement between the two curves. Whereas the values from μ CT image analysis are somewhat higher than that of from LOI test, especially in the third day.

Figure 3e) shows the derived pore structure of the specimen OPC_3d. Figure 3f) demonstrates the interconnected pore voxels corresponding to the pore structure shown in Figure 3e). The isolated pore voxels which are not connected to either the top or bottom surface are removed. These isolated pores make no contribute to transport properties of cement paste. The degrees of pore connectivity of the specimen at varying curing ages are 0.95, 0.85, 0.84 and 0.48 respectively. The degree of pore connectivity decreases sharply with the increase of curing age of cement paste, especially for the specimen OPC_28. This agrees very well with the general knowledge on the microstructural development of cement paste and the progress of hydration reaction over time. As we know, with the progress of cement hydration, the capillary porosity decreases and capillary pores becomes disconnected at a certain time. The obtained connected porosity of cement paste at 1 day, 3 days, 7 days and 28 days are 25.96%, 17.01%, 15.84% and 6.41% respectively. The results show good quantitative agreement with that presented in Ref. [Promentilla 2009], where the connected porosity (defined as effective porosity in [Promentilla 2009]) derived from the microtomography images of cement paste ($w/c=0.50$, image resolution= $0.5\text{ }\mu\text{m/voxel}$) with curing age of 2 days, 7 days and 28 days are 15%, 12% and 9% respectively and the corresponding degree of pore connectivity are 0.82, 0.75 and 0.59 respectively.

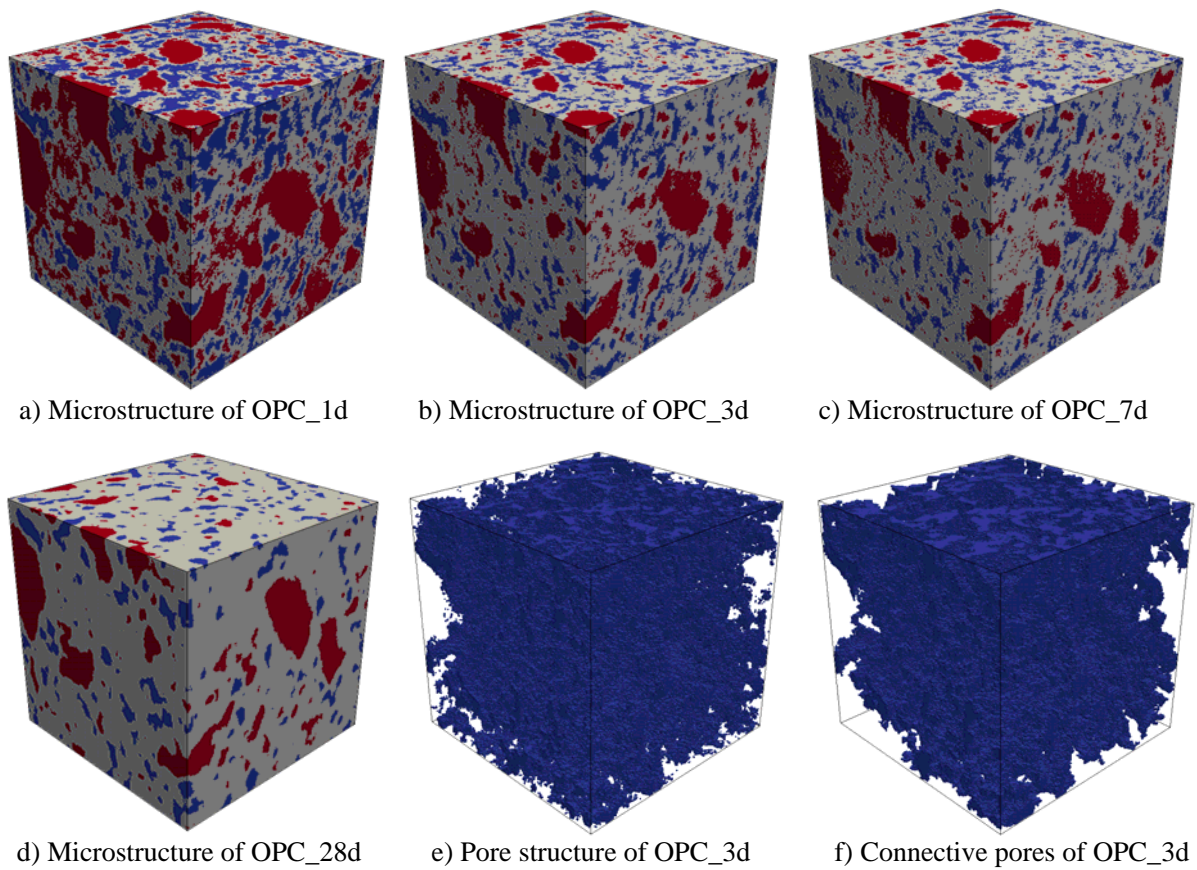


Figure 3: Visualization of the 3D reconstructed microstructure, pore structure and connective pore structure

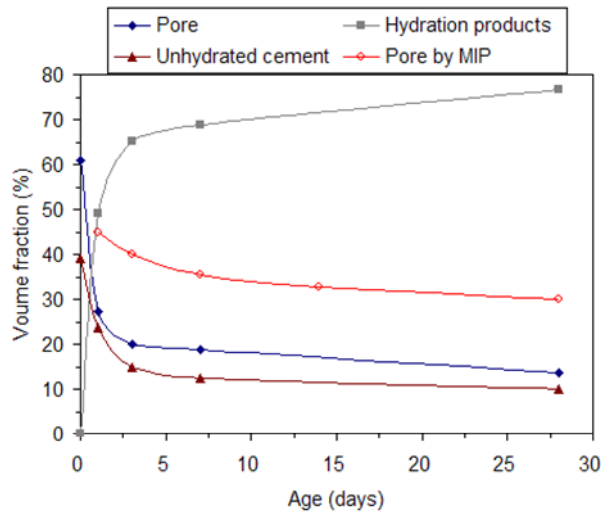


Figure 4: Volume fraction of phases at different age

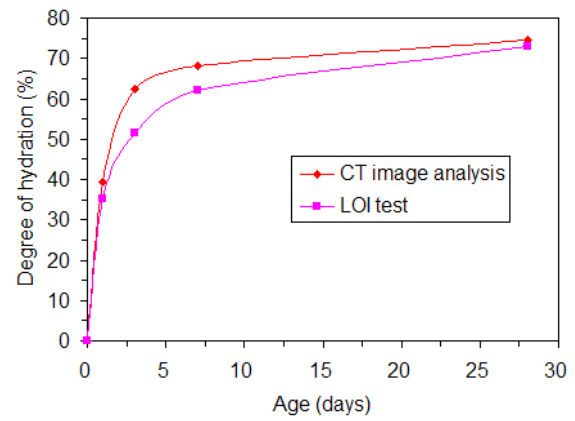


Figure 5: Degree of hydration as a function of age

Figure 6 shows the distribution of the concentration of tritiated water in the 3D pore network. The predicted tritiated water diffusion coefficients of the specimens at curing ages of 1, 3, 7 and 28 days are shown in Figure 7. The simulated value of 1.75×10^{-11} m/s corresponding to OPC_28d is about twice as much as the experimental value 9.50×10^{-12} m/s for Portland cement paste with w/c ratio 0.5 at

curing age of 28 days measured by Numata et al. [Numata 1990]. The little discrepancy between simulation and experiment may be attributed to the different chemical composition of the used cement.

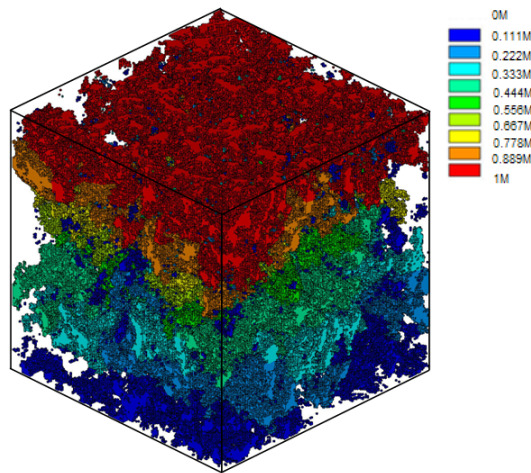


Figure 6: Concentration distribution of tritiated water in the 3D pore network

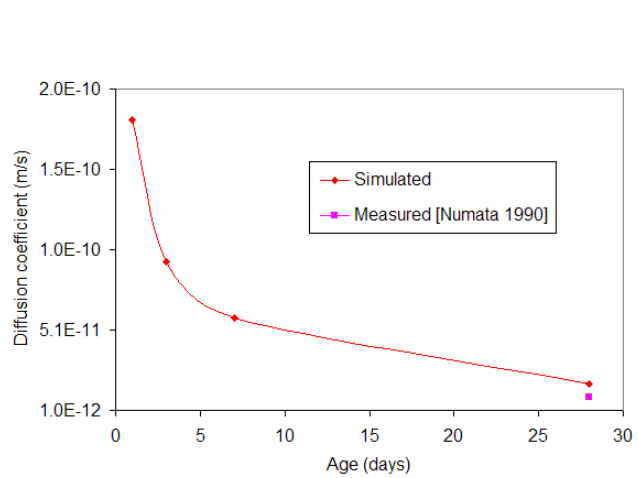


Figure 7: Effective diffusion coefficient as a function of curing age

4. Conclusions

This paper represents a procedure to investigate the microstructure evolution and predict the transport properties of hydrating cement paste based on the three-dimensional (3D) microtomography images acquired by using a high spatial resolution (0.5 $\mu\text{m}/\text{voxel}$) X-ray computed microtomography (micro-CT) technique. The 3D microstructure and pore network can be reconstructed after image processing and analysis. The volume fraction of pore voxels and the degree of hydration derived from CT image analysis show a good agreement with experimental results from MIP and LOI test, which indicates that micro-CT as a non-invasive technique is reliable and suitable to characterize the microstructure of hydrating cement paste. The obtained 3D microstructure of hydrating cement paste can be applied to predict the transport properties of cement-based materials.

References

- Feng X., Garboczi E.J., Bentz D.P. 2004. Estimation of the degree of hydration of blended cement pastes by a scanning electron microscope point-counting procedure. *Cement and Concrete Research* 34, 1787-1793.
- He Y.J., Mote J., Hu S.G., Lange D.A. 2010. Micro-CT study on microstructure evolution of cement paste.
- Hoshen J., Kopelman R. 1976. Percolation and cluster distribution. I. Cluster multiple labeling technique and critical concentration algorithm. *Physical Review B* 14, 3438-3445.
- Mills R. 1973. Self-diffusion in normal and heavy water in the range 1-45 °C. *The Journal of Physical Chemistry* 5, 685-688.
- Numata S., Amano H., Minami K. 1990. Diffusion of tritiated water in cement materials. *Journal of Nuclear Materials* 171, 373-380.
- Promentilla M.A.B., Sugiyama T., Hitomi T., Takeda N. 2009. Quantification of tortuosity in hardened cement pastes using synchrotron-based X-ray computed microtomography. *Cement and Concrete Research* 39, 548-557.
- Raymond A.C., Kenneth C.H. 1999. Mercury porosimetry of hardened cement pastes. *Cement and Concrete Research* 29, 933-943.
- Rougelot T, Burlion N., Bernard D., Skoczylas F. 2010. About microcracking due to leaching in cementitious composites: X-ray microtomography description and numerical approach. *Cement and Concrete Research* 40, 271-283.
- Zhang M.Z., Ye G., van Breugel K. 2010. A numerical-statistical approach to determining the representative elementary volume (REV) of cement paste for measuring diffusivity. *Materiales de Construcción* 60, 7-20.
- Zhang M.Z., Ye G., van Breugel K. 2011. Microstructure-based modeling of water diffusivity in cement paste. *Construction and Building Materials* 25, 2046-2052.